Heliyon 10 (2024) e38342

Contents lists available at ScienceDirect

Heliyon

journal homepage: www.cell.com/heliyon

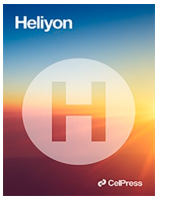

Research article

Construction of an endoplasmic reticulum stress and cuproptosis -related lncRNAs signature in chemosensitivity in hepatocellular carcinoma by comprehensive bioinformatics analysis

Xiao-Liang Qi [a,1], Gu-Qing Luo [a,1], Abudukadier Tuersun [b,1], Min Chen [a], Guang-Bo Wu [a], Lei Zheng [a], Hong-Jie Li [a], Xiao-Lou Lou [a,**], Meng Luo [a,*]

[a] Department of General Surgery, Shanghai Ninth People's Hospital Affiliated to Shanghai Jiao Tong University School of Medicine, Shanghai, China
[b] Department of General Surgery, Kashgar Prefecture Second People's Hospital of Xinjiang Uygur Autonomous Regions, Kashgar, Xinjiang, China

ARTICLE INFO

Keywords:
Hepatocellular carcinoma
Endoplasmic reticulum stress
Long non-coding RNA
Prognostic signature
Candidate drugs
Tumor immune microenvironment
Bioinformatics

ABSTRACT

Endoplasmic reticulum stress (ERS) and cuproptosis have remarkable effects on hepatocellular carcinoma (HCC) leading to a poor prognosis. The current study aimed to explore credible signature for predicting the prognosis of HCC based on ERS and cuproptosis-related lncRNAs. In our study, clinical and transcriptomic profiles of HCC patients were obtained from the Cancer Genome Atlas (TCGA) database. An ERS and cuproptosis-related lncRNA prognostic signature, including NRAV, SNHG3, LINC00839 and AC004687.1, was determined by correlation tests, Cox regression analysis, least absolute shrinkage, and selection operator (LASSO) methods. Survival and predictive value were evaluated using Kaplan–Meier and receiver operating characteristic (ROC) curves, while calibration and nomograms curves were developed. Besides the enrichment analyses for ERS and cuproptosis-related lncRNAs, mutational status and immune status were assessed with TMB and ESTIMATE. Additionally, consensus cluster analysis was employed to compare cancer subtype differences, while drug sensitivity and immunologic efficacy were evaluated for further exploration. qRT-PCR and CCK-8 were utilized to verify the alteration of the prognostic lncRNAs expression and proliferation in vitro. High-risk groups exhibited poorer prognosis. The signature exhibited robust predictive value as an independent prognostic indicator and showed significant correlation with clinicopathological features. In the enriched analysis, biological membrane pathways were enriched. Low-risk patients had lower TMB and higher immune status. A cluster analysis revealed that cluster 2 had the best clinical immunological efficacy and most active immune function. In brief, our constructed signature with ERS and cuproptosis-related lncRNAs was associated survival outcomes of HCC, and can be used to predict the clinical classification and curative effect.

* Corresponding author. Shanghai Ninth People's Hospital Affiliated to Shanghai Jiao Tong University School of Medicine, No.639, Zhi Zao Ju Road, Shanghai, 200011, China.
** Corresponding author. Shanghai Ninth People's Hospital Affiliated to Shanghai Jiao Tong University School of Medicine, No.639, Zhi Zao Ju Road, Shanghai, 200011, China.
E-mail addresses: lou_xl@163.com (X.-L. Lou), luosh9hospital@sina.com (M. Luo).
[1] These authors contributed equally to this work.

https://doi.org/10.1016/j.heliyon.2024.e38342
Received 19 December 2023; Received in revised form 22 September 2024; Accepted 23 September 2024
Available online 24 September 2024

1. Introduction

Hepatocellular carcinoma (HCC), the predominant subtype of liver cancer, is responsible for more than 90 % of all deaths caused by this disease [1]. Currently, surgery is the main effective therapy for HCC. Nevertheless, individuals who experience rapid advancement and have a high level of severity frequently miss out on the chance for surgical intervention. Furthermore, as a result of the HCC features, individuals with distant metastasis frequently experience an unfavorable outlook [2], with a mere 18.1 % survival rate over a span of five years. Therefore, a comprehensive comprehension of the development and advancement of HCC is crucial for enhancing clinical outcomes and providing more efficient therapies.

Endoplasmic reticulum (ER), the largest organelle of eukaryotic cells, has a function to modify nutrient and synthesize protein, lipid and steroid [3]. Disorders caused by physiological or pathological stress, such as imbalances in iron levels, deficiencies in nutrition, and etc, have the potential to disrupt the process of protein synthesis or modification in the ER. This disruption can trigger the accumulation of misfolded proteins and an increased burden on the ER [4,5]. Cell homeostasis is maintained through the participation of three sensors, namely PRKR-like ER kinase (PERK), inositol requiring enzyme 1 (IRE1), and activating transcription factor 6 (ATF6), which are primarily linked to Endoplasmic reticulum stress (ERS) [6]. Importantly, ERS was considered as a vital driver of malignant tumorigenesis [7]. Excessive protein production from ERS accelerates the abnormal cell proliferation related to development of solid tumors [8]. Studies have found that GSK 2656157, the blocker of ERS, had an efficiently suppression on malignancy growth [9]. In HCC patients, ER stress was linked to tumorigenesis, development, metastasis, angiogenesis and drug resistance [10]. To benefit more malignant patients, in-depth mechanisms of ERS is essential to figure out, which help human beings to develop further clinical therapies.

Cuproptosis is a new programmed cell death firstly published in 2022 [11]. It was highlighted that the intracellular accumulation of copper would lead to aggregation of lipoylated dihydrolipoamide S-acetyltransferase (DLAT), which led to toxic protein stress and eventually resulted in cell death [12]. Copper metabolism is crucial in tumorigenesis and tumor therapeutics [13–15]. Furthermore, it was also reported that copper and copper-related cuproptosis were related to tumor microenvironment and prognostic prediction of HCC [16,17].

Overwhelming evidence has suggested the tight relationship between ERS and cuproptosis. Kong et al. has reported the improvement of copper transport by ERS inhibition in hepatic stellate cells under copper load, which suggested a potentially synergistic effect of ERS and cuproptosis during disease progression [18]. Moreover, copper can also induce inflammation and apoptosis through activation of ERS [19,20]. Therefore, the effects of both ERS and cuproptosis on HCC warrant further exploration.

According to Refs. [21,22], a long non-coding RNA (lncRNA) exceeds 200 nucleotides but is not capable of encoding proteins. Earlier research has discovered their involvement in the control of cancer signaling pathways [23,24]. They participated in the procession of ERS and protected cardiomyocytes from ERS via miR-6324 in myocardial infarction [25]. LncRNA MEG3 initiated ERS through the MEG3/miR-103a-3p/PDHB axis in colorectal carcinoma [26]. However, the mechanisms by which ERS and cuproptosis regulate HCC progression through lncRNAs remain unclear. We propose that lncRNAs linked to ERS and cuproptosis might predict prognosis, providing a theoretical basis for precise therapies.

This study involved the creation of a predictive pattern using ERS and cuproptosis-associated lncRNAs and examined the variation in prognosis associated with the pattern for investigating the significance of ERS in HCC. The workflow was presented in Supplementary Fig. 1. Our objective was to elucidate the function of ERS and cuproptosis-associated lncRNAs in HCC, with the aspiration that this ongoing investigation may offer a fresh perspective on the clinical prognosis and therapy of HCC.

2. Methods

2.1. Public data acquisition

Data from the TCGA-LIHC (https://www.cancer.gov/ccg/research/genome-sequencing/tcga) were obtained, including RNA-seq and clinical profiles. Exclusion was done for patients lacking comprehensive clinical or survival data. Patients with a follow-up duration of more than one month were included in the subsequent analysis. Ensembl was the source of the gene transfer format (GTF) files, which were used to distinguish between messenger RNAs (mRNAs) and lncRNAs [27]. In the meantime, 314 genes, which were also protein-coding genes (PCG), related to ERS and cuproptosis (Supplementary Table 1) were identified from the Gene Set Enrichment Analysis (GSEA) dataset and previous literature [28–34].

2.2. Identification of lncRNAs associated with ERS and development of a prognostic risk signature

All gene expression data was pre-prepared and a gene expression matrix was generated via R package. To identify ERS and cuproptosis-associated lncRNAs, the criterion used was a Pearson correlation coefficient ($|cor|$) > 0.5 and a *P*-value <0.001. Using a threshold [$|\log2$ fold change (FC)| >1 and false discovery rate (FDR) < 0.05], 127 lncRNAs associated with ERS and cuproptosis were identified as differential expression between normal and tumor tissue (Supplementary Table 2). The expression profile of those lncRNAs in TCGA-LIHC samples was uploaded as Supplementary Table 3. Next, a univariate Cox regression analysis was employed to identify ERS and cuproptosis-related lncRNAs that showed a significant association with the clinical prognosis in HCC patients ($P <$ 0.05). We further refined the lncRNA selection by using LASSO Cox regression to avoid overfitting. Then, the Akaike Information Criterion (AIC) value for ERS and cuproptosis-associated lncRNAs was calculated using multivariate Cox proportional hazards regression [35]. The following formula was used to calculate the risk score of each HCC patient:

$$\text{Risk Score} = \sum_{k=1} \text{Coef(k)}*\text{E(k)}$$

The regression coefficient for prognostic ERS and cuproptosis-related lncRNAs was represented by Coef (k), while lncRNAs levels were represented by E(k). To classify HCC patients into high- and low-risk groups, the cutoff value was determined on the basis of the median risk score.

2.3. Analysis of survival and consensus clustering

To construct survival plots in various subgroups, the relationship between the risk prognostic signature in subgroups and the survival status was estimated using Kaplan-Meier plot and Log rank tests. Due to close association with genetic mutations in HCC patients, we analyzed the several mutations between both subgroups. Next, we assessed the risk prognostic signature for predictively prognostic value using time-dependent receiver operating characteristic (ROC) curves. In conclusion, consensus clustering was conducted to identify the optimal number of clusters based on the identified ERS and cuproptosis-associated lncRNAs.

2.4. Analysis of genetic mutations and enrichment of gene sets

We examined the mutation status in various subcategories and represented the findings using waterfall plots. To determine the distinctions between pathways and biological processes in subgroups, we conducted GSEA using Kyoto Encyclopedia of Genes and Genomes (KEGG) and gene ontology (GO) analysis through the differential PCGs that obtained from the risk prognostic model. We examined the important items using a P value < 0.05 after making adjustments.

2.5. Assessment of immune status calculation and infiltration

To estimate the immune status of each sample, the immune and stromal scores were calculated in the TCGA cohort via the ESTIMATE algorithm. The verification of the correlation between stromal and immune scores and risk scores was conducted using Pearson analysis. Additionally, the influence of the risk predictive signature on immunotherapies was further demonstrated by examining the correlation between risk score and established immune checkpoint genes [36]. Subsequently, the association between tumor-infiltrating immune cells and prognostic signature was evaluated by quantifying the ratios of tumor-infiltrating immune cells [37].

2.6. Prediction of immunotherapy and chemotherapy susceptibility

Using the Tumor immune dysfunction and exclusion (TIDE) algorithm and subclass mapping, we evaluated cytotoxic T lymphocyte-associated protein 4 (CTLA4) immune checkpoint effectiveness and programmed cell death ligand 1 (PD-1) across different subgroups [38,39]. The pRRophetic R package was employed for predicting the response of the TCGA cohort to five chemotherapeutic agents by calculating the semi-maximum inhibitory concentration (IC50).

2.7. Biological function assay

Human immortalized liver cell line, HepaRG, and HCC cell line, HepG2, culturing in DMEM medium (Gibco, USA) containing 10 % FBS (Gibco, USA) at 5 % CO2, 37 °C, were sourced from the Chinese Academy Sciences (Shanghai, China). HepaRG cells exhibit certain properties and features to adult hepatocytes, unlike in vitro primary human hepatocytes (PHH) [40]. Human hepatoma HepG2 cells are mainly utilized for research on metabolism and hepatotoxicity [41]. Cell toxicity was evaluated by the Cell Counting Kit-8 (CCK-8). 96-well plates were used to combine 1×10^5 HCC cells with the CCK-8 working solution. In addition, the cells in the experimental group were subjected to treatment with 1 mm Dasatinib [42]. Subsequently, the absorbance of 50 nm was observed at 0 h, 12 h, 24 h, 48 h, and 72 h in a repetitive manner. Finally, the information was gathered and presented in a visual format.

2.8. Real-time quantitative polymerase chain reaction

TRIzol RNA extraction kit (TaKaRa) was used to extract total RNA followed by reverse transcription with Prime-Script Reverse Kit (TaKaRa). Gene expression levels were quantified using SYBR Green. The primers used in the process were as follows: NRAV (Forward) - 5′- GGAGTTGATGCCTCCGAACA-3′ and (Reverse) - 5′- ATGACCGGAGCTGAAAGGTG-3’; SNHG3 (Forward) - 5′-TTCAAGCGATTCTCGTGCC-3′ and (Reverse) - 5′-AAGATTGTCAAACCCTCCCTGT-3′; LINC00839 (Forward) - 5′-CAGGTCCTGAAATCAGCCTTG-3′ and (Reverse) - 5′-GCAGTTTCCACATTTGAAACCA-3’. AC004687.1 (Forward) - 5′-AGACAGACAGTGCAGTCACC-3′ and (Reverse) - TCTCCGAAGCCCACAGTACA-3′; GAPDH (Forward) - 5′- GGAGCGAGATCCCTCCAAAAT-3′ and (Reverse) - 5′- GGCTGTTGTCATACTTCTCATGG-3’.

2.9. Statistics

GraphPad Prism v8.00 and tools-R software were utilized for the completion of all statistical analysis. In statistics, a P-value below

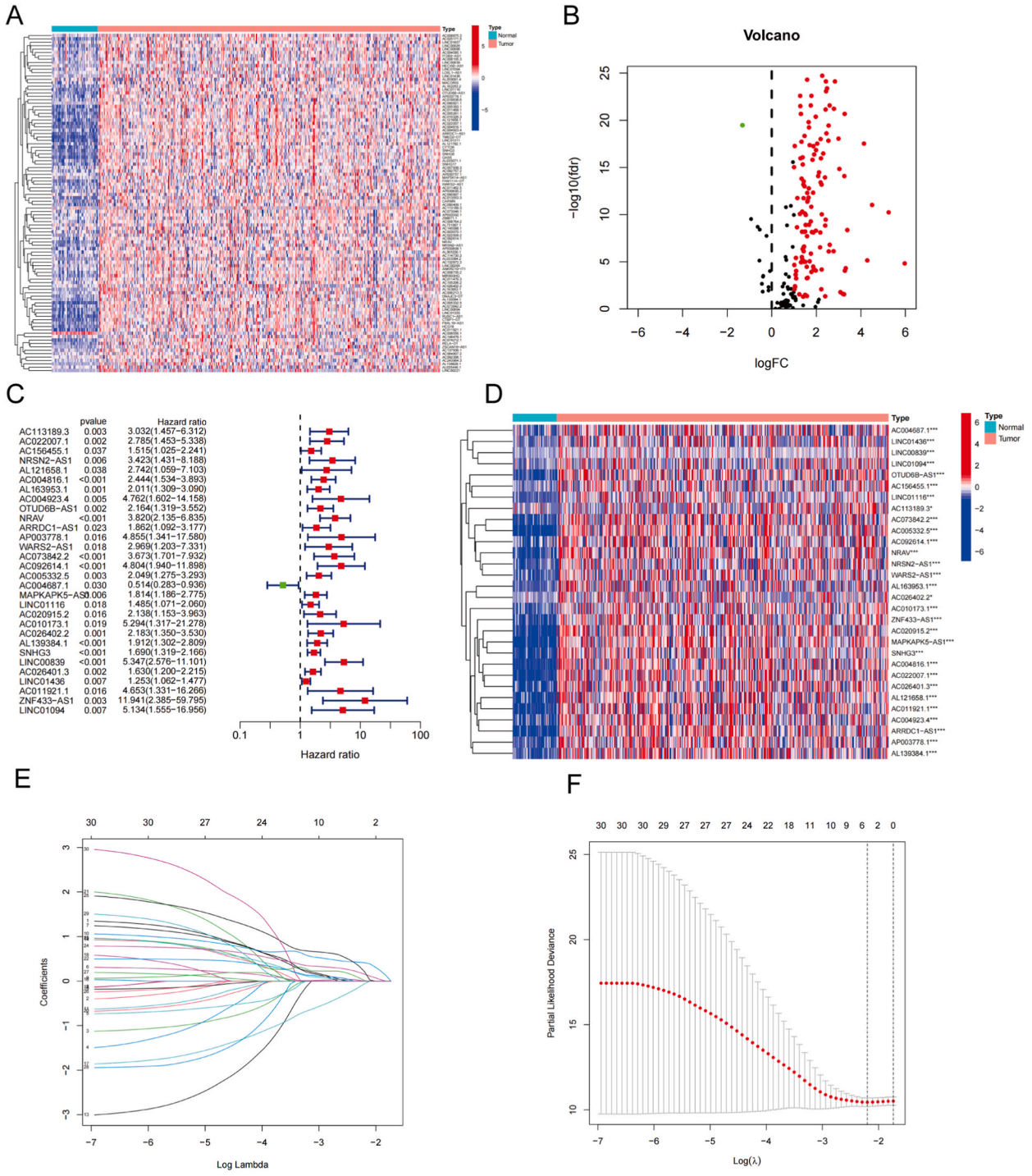

Fig. 1. Identification of the prognostic ERS and cuproptosis-related lncRNAs in HCC.
(A) All differentially expressed lncRNAs in Heatmap. (B) Upregulated ERS and cuproptosis-related lncRNAs (Red dots) and downregulated ERS and cuproptosis-related lncRNAs in volcano plot. The prognostic ERS and cuproptosis-related lncRNAs screened through the univariate Cox regression analysis via forest plot (C) and heatmap (D), respectively. LASSO variable trajectory plot across 1000 cross-validations (E) and LASSO coefficient profile (F), respectively.

0.05 was considered as statistically significant.

3. Results

3.1. Identification of the prognostic ERS and cuproptosis-related lncRNAs in HCC patients

After preparing raw data from TCGA database, all cases whose survival time was lacking or under 30 days were removed in subsequent analysis. After conducting Pearson correlation analysis, ERS and cuproptosis-related lncRNAs were filtered out from TCGA database and further prepared through the differential expression between tumor and normal tissue, containing 127 ERS and cuproptosis-related lncRNAs. There was a differential expression observed between the tumor and adjacent tissue, with an absolute log2 fold change greater than 1 and a false discovery rate less than 0.05. The lncRNAs were displayed in a heatmap (Fig. 1A), while the volcano plot illustrated the distribution of all upregulated and downregulated lncRNAs in tumor tissue (Fig. 1B).

3.2. Construction and verification of the ERS and cuproptosis-related lncRNA prognostic signature

During the preprocessing stage, a univariate Cox regression was conducted to extract a set of 30 lncRNAs that were associated with the prognosis of HCC and were related to ERS and cuproptosis. Fig. 1C presented Hazard Rates (HR) and the significance of expression (*P* value) for the results. HR value of all lncRNAs, except AC004687.1, was over 1, which mean that those lncRNAs might act as risk factors. Next, the heatmap (Fig. 1D) displayed the expression patterns of a combined 30 lncRNAs associated with ERS and cuproptosis. By analyzing the heatmap, it becomes evident that all lncRNAs exhibited a notable upregulation in tumor tissue. Afterwards, the LASSO technique was employed to penalize all lncRNAs associated with ERS and cuproptosis (Fig. 1E and F), followed by the execution of multivariate Cox regression. In conclusion, we have determined that NRAV, AC004687.1, SNHG3, and LINC00839 were the most suitable lncRNAs for developing a risk signature as prognostic biomarkers. For better understanding the influence of ERS and cuproptosis on HCC patients, the patients were categorized into high-risk and low-risk subgroups based on the threshold, which was determined as the median of the risk score. The risk score was derived from each lncRNA level and the correlation coefficient from the multivariate Cox regression analysis. Heatmaps and scatter plots were completed to compare the variation in expression, survival status, and risk score ranking distribution among different risk subgroups. This analysis was performed using 4 lncRNAs prognostic biomarkers in the training, validation, and complete sets (Fig. 2A–C). In the high-risk subgroup, NRAV, SNHG3, and LINC00839 exhibited significant expression levels and displayed a consistent expression pattern, excluding AC004687.1. Furthermore, with the escalation of the risk score, a corresponding rise in mortality rates was observed, suggesting a link between HCC risk scores and survival. Furthermore, the Kaplan-Meier survival plots demonstrated a notable disparity in survival rates between the high- and low-risk groups of HCC patients (Fig. 3A–C) within the training, validation, and complete sets. This finding further validates the prognostic significance of the risk prognostic signature.

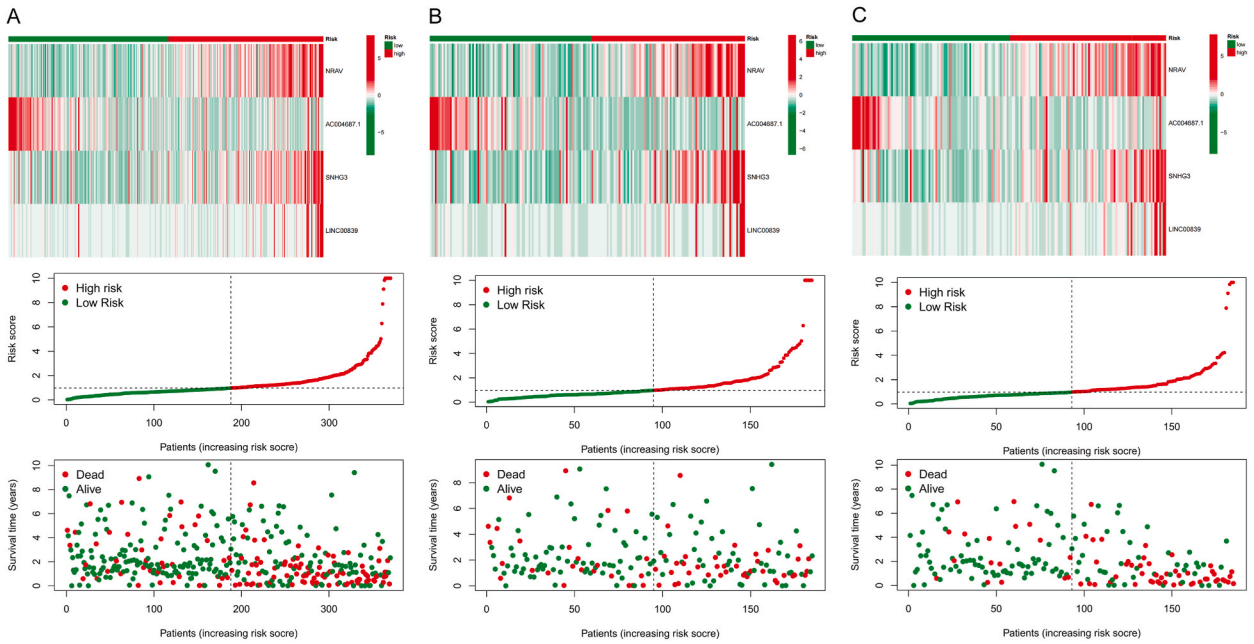

Fig. 2. The risk analysis of 4 ERS and cuproptosis-related lncRNAs in subgroups for HCC patients.
Expression heatmap, risk score distribution and scatter plots of 4 ERS and cuproptosis-related lncRNAs in the training (A), validation (B) and complete group (C).

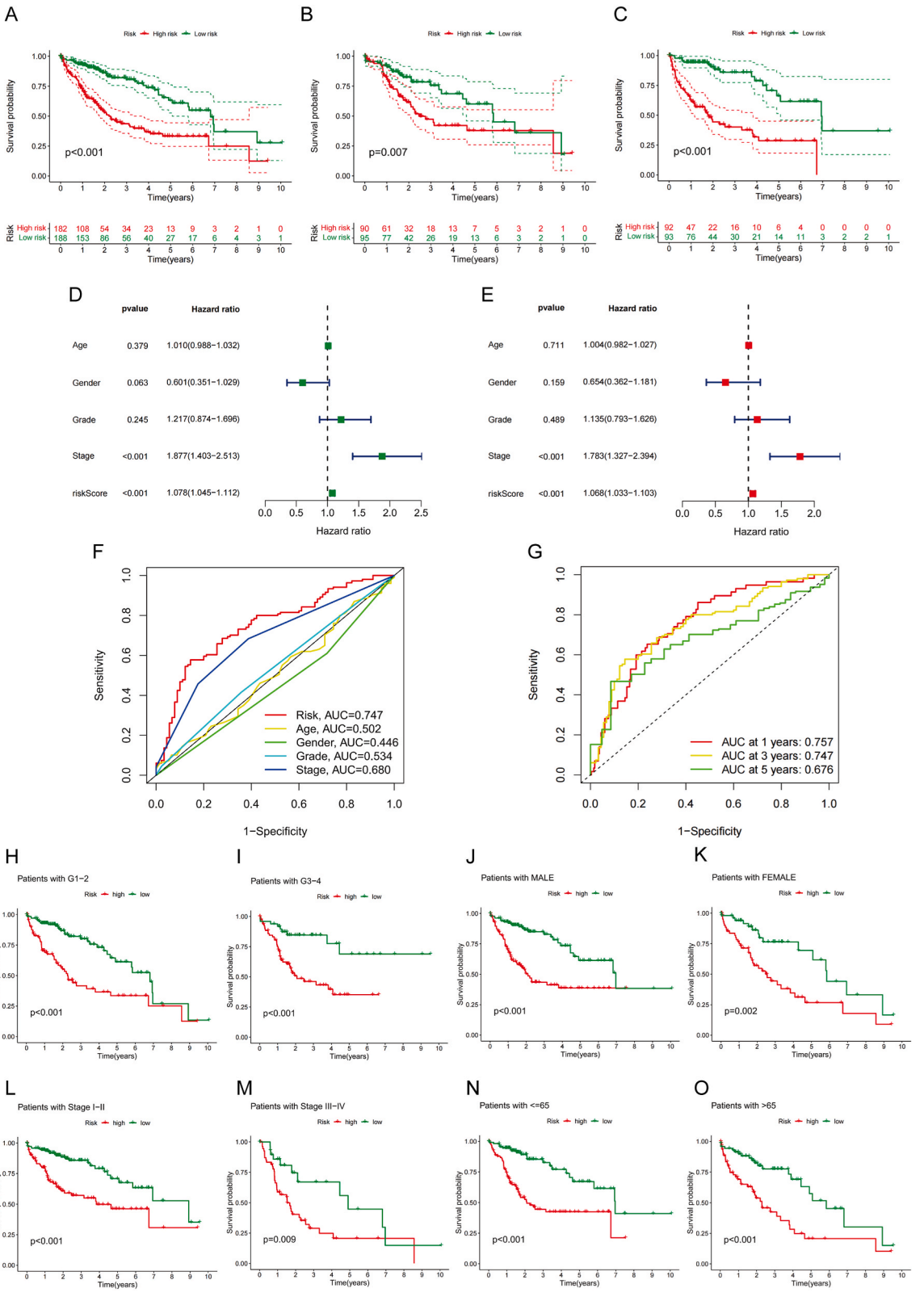

(caption on next page)

Fig. 3. The validation of the ERS and cuproptosis-related lncRNAs prognostic signature and its association with clinical features.
Survival plots of 4 ERS and cuproptosis-related lncRNAs in the training (A), validation (B) and complete group (C). Univariate (D) and multivariate (E) independent Cox regression analysis of clinicopathological characteristics and the risk score. (F) ROC and AUC curves of clinicopathological features and the risk score. (G) ROC and AUC curves of 1-, 3- and 5-year survival rates of the complete set. H-O: The Kaplan-Meier survival curves of two risk subgroups on the clinical features in the completes set.

Additionally, to validate if the risk prognostic signature can function as a standalone prognostic model for patients with HCC, the univariate Cox regression revealed that the risk signature and stage served as autonomous indicators ($P < 0.001$) (Fig. 3D) and the multivariate Cox regression confirmed that both the risk signature and stage were autonomous indicators in the univariate Cox

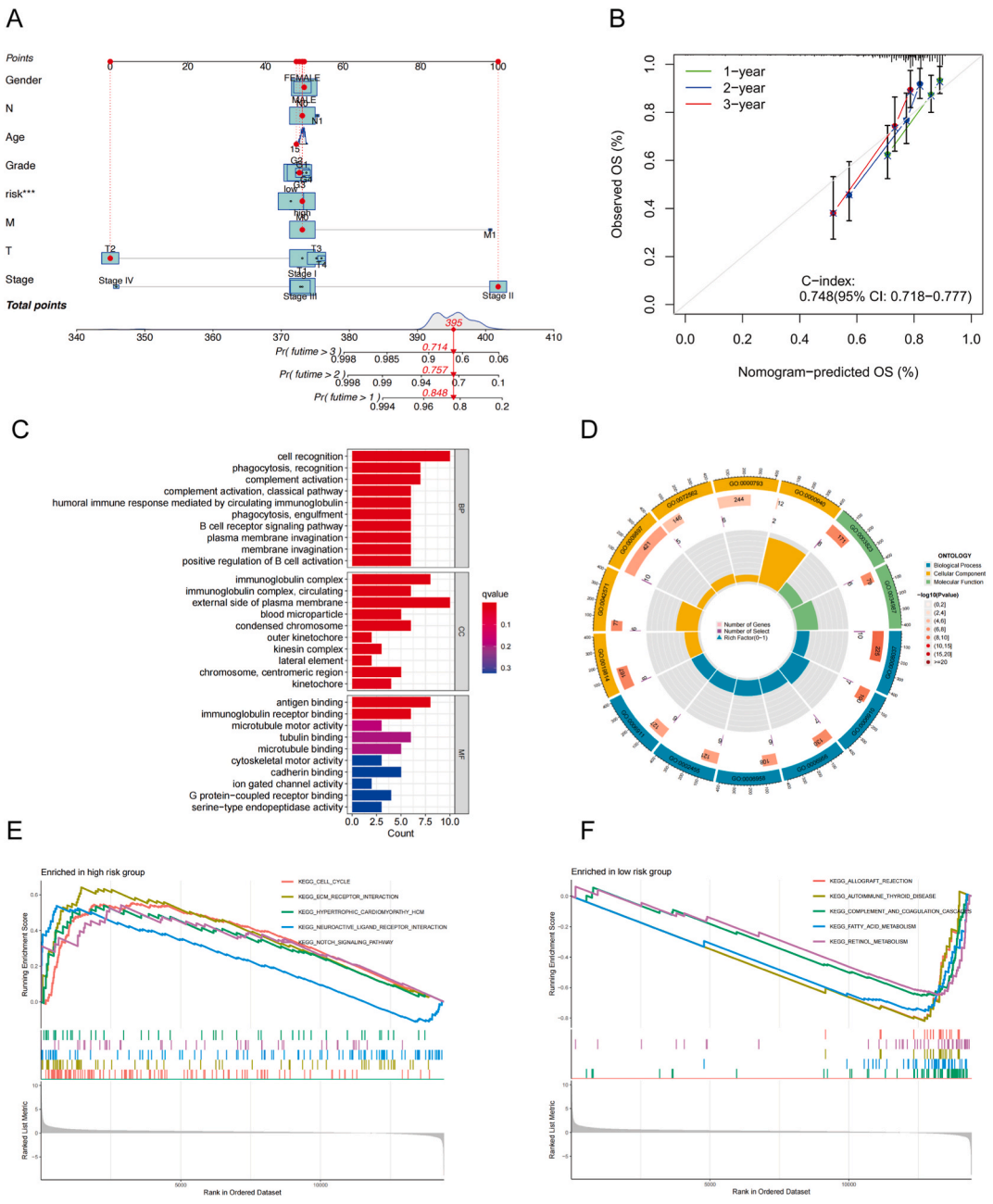

Fig. 4. Construction of the nomogram and exploration of biological pathways.
(A) nomogram model of clinicopathological features in HCC patients. (B) The relationship between the observed OS at 1-, 3- and 5-years and the combined risk score. The GO analysis in bar plots (C) and its distribution of genes in circle plot (D). The GSEA analysis in high- (E) and low-risk subgroup (F), respectively.

regression ($P < 0.001$) (Fig. 3E). To conduct additional predictive analysis, the risk prognostic signature was evaluated using ROC and AUC curves to assess its predictive capability. The risk score's AUC value was 0.747, surpassing that of age, grade, gender, and stage (Fig. 3F). In the meantime, the AUC values for forecasting the survival rates of one, three, and five years were 0.757, 0.747, and 0.676, correspondingly, as shown in Fig. 3G, which exhibited remarkable ability to predict risk in the present investigation. Regarding the

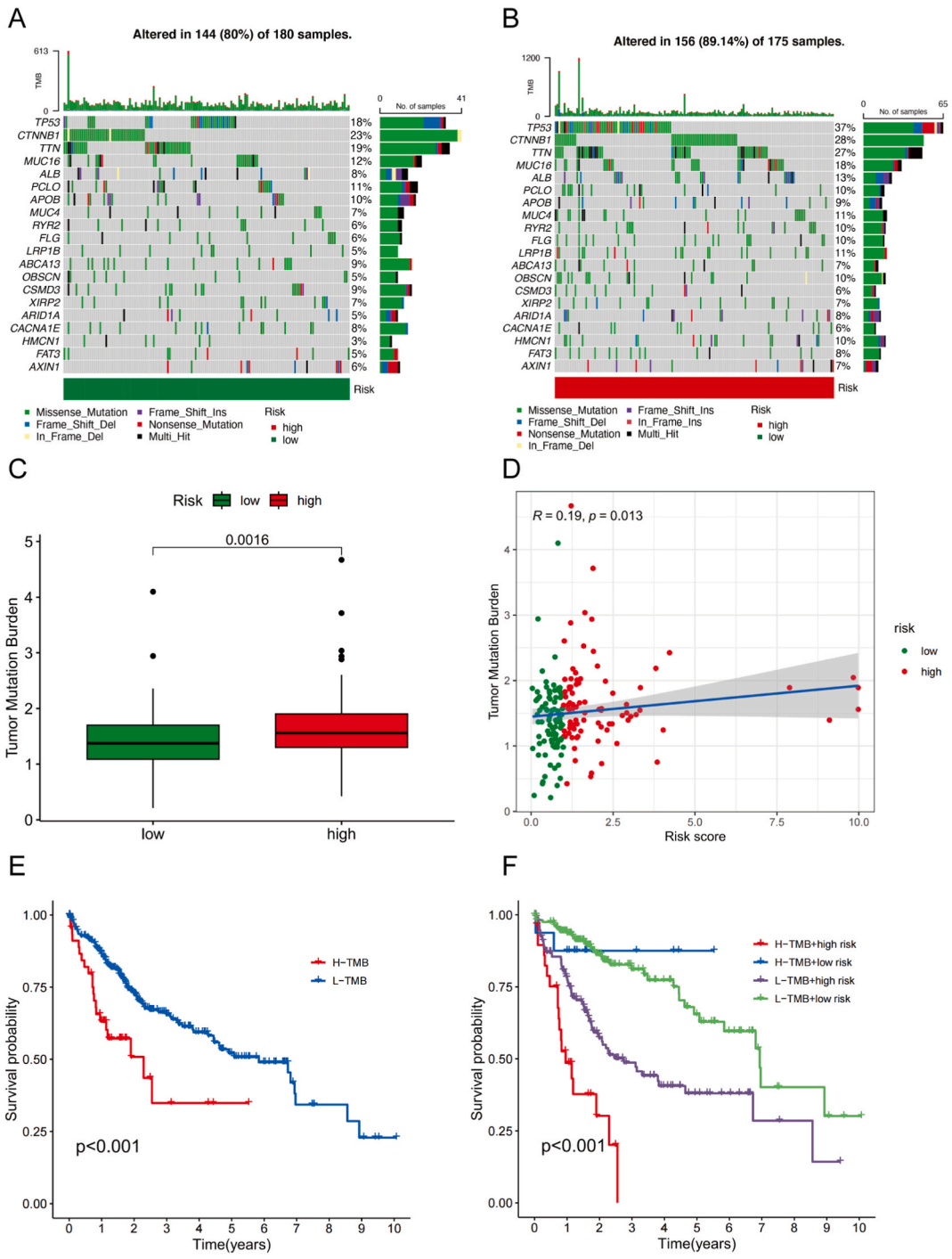

Fig. 5. TMB analysis of the risk prognostic signature.
The waterfall plots of tumor mutation profiles in high- (B) and low-risk (A) subgroups. (C) The difference of TMB between high-risk and low-risk subgroups in a bar plot. (D) The correlation between TMB and risk score. (E) Kaplan-Meier curves of HCC patients in the H-TMB and L-TMB subgroups. (F) Kaplan–Meier plots of HCC patients in various subgroups (H-TMB + high risk, H-TMB + low risk, L-TMB + high risk and L-TMB + low risk).

correlation between clinicopathological characteristics and prognostic risk, it was observed that patients in the high-risk subgroup exhibited diverse clinicopathological features such as stage, gender, grade, and age, which ultimately led to a poorer clinical outcome in comparison to the low-risk subgroup ($P < 0.001$) (Fig. 3H–O). The results kept in line with the above independence analysis.

4. Construction of the nomogram and exploration of biological pathways

We created a nomogram (Fig. 4A) to merge the risk score and clinical characteristics for validating the prognostic ability of 1-, 3-, and 5-year overall survival (OS) predictions. Fig. 4B indicated that the nomogram-predicted OS and the observed OS exhibited remarkable similarity, as indicated by the calibration curves. Next, in order to determine the biological progression of ERS and cuproptosis-associated lncRNAs, we conducted an analysis of GO and GSEA. According to the data presented in Fig. 4C and D, the findings of the biological processes (BP) demonstrated that ERS and cuproptosis-associated lncRNAs were predominantly concentrated in cell identification, recognition of phagocytosis, and activation of complement. ERS and cuproptosis-associated lncRNAs were predominantly concentrated in the outer surface of the cell membrane, immunoglobulin complexes, and compacted chromosomes within the cellular components (CC). ERS and cuproptosis-associated lncRNAs were predominantly enriched in antigen binding, binding to immunoglobulin receptors, and binding to tubulin in terms of molecular functions. During the GSEA analysis, the high-risk subgroup showed greater enrichment scores in the cell cycle, interaction with extracellular matrix (ECM) receptors, hypertrophic cardiomyopathy (HCM), interaction with neuroactive ligand receptors, and the Notch signaling pathway (Fig. 4E). Additionally, we discovered that the low-risk subgroup exhibited significant enrichment in allograft rejection, complement and coagulation cascades, autoimmune thyroid disease, fatty acid metabolism, and retinol metabolism (Fig. 4F).

5. The correlation between tumor mutation burden and the ERS and cuproptosis-related lncRNAs signature

To investigate the mutation profile in HCC patients, including all 355 cases, the mutation frequencies in two subgroups was calculated and represented in waterfall plots (Fig. 5A and B). In the high-risk subgroup, the mutation frequency was 89.14 %, whereas it was 80 % in the low-risk subgroup. The findings indicated that TP53, CTNNB1, TTN, MUC16, ALB, PCLO, and APOB were the primary genes that underwent mutations in the two subcategories. The mutation frequencies of the aforementioned mutated genes were significantly greater in the high-risk subgroup compared to the low-risk subgroup. Subsequently, the TMB examination demonstrated that individuals with HCC in high-risk categories exhibited a notably elevated TMB compared to those in the low-risk category ($P = 0.0016$, Fig. 5C). The relationship between two subcategories indicated that TMB had a significant positive correlation with the risk score ($R = 0.19$, $P = 0.013$, Fig. 5D). Furthermore, the findings from Kaplan-Meier diagrams of TMB revealed that HCC cases in the high-risk category experienced a more unfavorable outcome compared to those in the low-risk category ($P < 0.001$, Fig. 5E). In the meantime, the findings from a multigroup analysis combining risk and TMB indicated that patients with a low-risk profile and low TMB exhibited the most favorable survival outcome (Fig. 5F).

6. Exploration of the tumor immune status in two subgroups

Considering the critical role of ERS and cuproptosis in immune system, we conducted additional investigation into the immune condition of the tumor by analyzing the scores of the tumor microenvironment, including the StromalScore, ImmuneScore, and ESTIMATEScore. According to the findings, the scores of tumor microenvironment in the high-risk subgroup were significantly reduced compared to those in the low-risk subgroup (Fig. 6A–C). Moreover, we assessed the variations in immune infiltration within two distinct subcategories. Based on the data presented in Fig. 6D, we observed that there was a wide distribution of negative correlation coefficients, suggesting that individuals with a higher classifier index exhibited signs of immunosuppression. The classifier index showed a negative correlation with mast cell, $CD4^+$ memory T cell, common lymphoid progenitor, and $CD4^+$ Th2 T cell in XCELL, Neutrophil, and macrophage in TIMER, Macrophage M2, monocyte, and non-regulatory $CD4^+$ T cell in QUANTISEQ, macrophage/monocyte in MCPCOUNTER, uncharacterized cell in EPIC, Neutrophil, macrophage M0, and NK resting cell in CIBERSORT-ABS. On the other hand, neutrophil, NK resting cell, macrophage M2, and macrophage M0 in CIBERSORT were positively correlated with the classifier index in various algorithms. Furthermore, we evaluated the influence of predominantly immune cells on the survival of HCC through Kaplan-Meier plots. These immunocytes include $CD8^+$ T cells, $CD4^+$ memory resting T cells, Neutrophil (TIMER), Neutrophil (CIBERSORT), Neutrophil (CIBERSORT-ABS), Monocyte, Macrophage M1, Macrophage M0 (CIBERSORT), and Macrophage M0 (CIBERSORT-ABS) (Fig. 6G). In terms of immunocyte infiltration, excluding $CD4^+$ memory resting T cells and $CD8^+$ T cells, individuals in high-risk subgroups exhibited a significantly worse prognosis ($P < 0.05$). In the meantime, a correlation analysis was performed between ssGSEA enrichment scores and immunocyte subsets and functions. According to the findings, the majority of immune-related cells exhibited elevated ssGSEA scores in low-risk individuals, except for macrophage and immature dendritic cells (ICDs) ($P < 0.05$) (Fig. 6E). Likewise, the findings regarding immune functions revealed that major histocompatibility complex (MHC) class I exhibited no significant statistical importance, whereas the other function in the low-risk subgroup displayed significantly higher levels compared to the high-risk subgroup (Fig. 6F). As a result, it stimulated the immune activity in the subgroups with low risk.

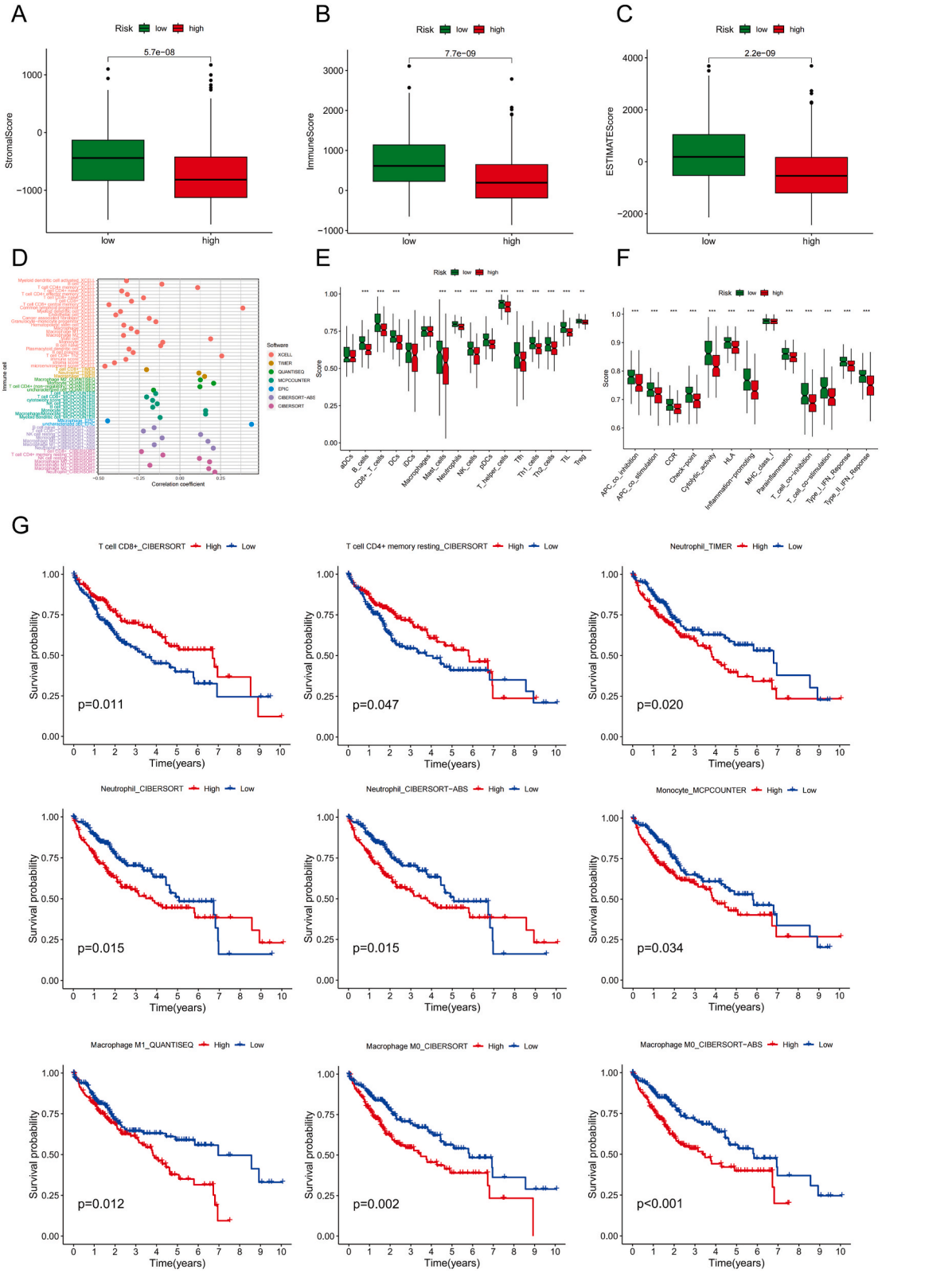

(caption on next page)

Fig. 6. Summary of the tumor immune status in two subgroups.
The boxplots of StromalScore (A), ImmuneScore (B) and ESTIMATEScore (C) in high- and low-risk subgroups. (D) Estimation of immune-infiltrating cells through the Spearman correlation analysis. The comparation of the infiltrating immune cells (E) and immune-related functions (F). (G) Kaplan-Meier plots of $CD4^+$ memory resting T cells, $CD8^+$ T cells, Neutrophil (TIMER), Neutrophil (CIBERSORT), Neutrophil (CIBERSORT-ABS), Monocyte, Macrophage M1, Macrophage M0 (CIBERSORT) and Macrophage M0 (CIBERSORT-ABS).

7. Consensus clustering analysis of ERS and cuproptosis-related lncRNAs and the difference of immune status in consensus cluster

Consensus clustering analysis was performed to ascertain the involvement of these lncRNAs in the onset and progression of HCC. In consensus clustering results (Fig. 7A), selecting $k = 2$ resulted in the most stable aggregation. This choice divided all tumor cases into two clusters, namely cluster 1 and cluster 2. Subsequently, a notable distinction in operating system (OS) was noted between the two clusters, with cluster 2 demonstrating a more favorable prognosis compared to cluster 1 ($P < 0.001$, as shown in Fig. 7B). According to the Sankey diagram in Fig. 7C, cluster 1 consisted of predominantly high-risk patients, while cluster 2 primarily comprised low-risk patients. Subsequently, the tSNE analysis revealed distinct dimensions among the subgroups with high and low risk (Fig. 7D). Equally, tSNE analysis between distinct clusters was performed and showed different dimensions as well (Fig. 7E). Furthermore, in order to determine the disparity in immune response between the two clusters, a heatmap illustrating the immune response was generated, revealing a higher abundance of immune cell infiltration in cluster 1 (Fig. 7F). Furthermore, in terms of the significance of immunotherapy, a comparison was made between two clusters regarding the expression of conventional immune checkpoint molecules (Fig. 7G). The findings suggested that CD276 exhibited the greatest level of expression in both cluster 1 and cluster 2, whereas BTNL2 displayed the lowest level of expression in both cluster 1 and cluster 2. We noticed a significant difference in the expression of classical immune checkpoint molecules, with almost all immune checkpoint molecules being more highly expressed in cluster 1. Fortuitously, BTNL2 and HHLA2 had higher expression in cluster 2, whose expression was extremely low.

8. The sensitivity analysis of potential clinical drugs and the validation of prognostic lncRNAs

The potential of broad studies has generated significant interest in the use of immunotherapy and targeted treatments for patients with HCC, offering a solid basis for clinical application using the existing prognostic risk signature in potential high-risk medications. We conducted a comparative evaluation of drug sensitivity using IC50 to analyze the sensitivity of six potential target drugs (Axitinib, Afatinib, Gefitinib, Dasatinib, Crizotinib, and Lapatinib) in various risk subgroups and clusters (Fig. 8A and B). Patients with HCC in the high-risk category exhibited greater responsiveness to Axitinib, which demonstrated higher effectiveness in patients belonging to the C1 cluster. It's worth mentioning that HCC patients in the low-risk category exhibit higher responsiveness to Afatinib, Gefitinib, Dasatinib, Crizotinib, and Lapatinib. This aligns with the vulnerability observed in the C2 cluster of HCC patients. Therefore, patients with HCC in the low-risk subgroup or C2 cluster have a higher likelihood of experiencing the development of targeted medications. To identify potential immunotherapeutic medications, the investigation examined the expression of immune checkpoint genes in various risk subcategories (Fig. 8C). In the high-risk subgroup, CD276 and NRP1 exhibited relatively elevated expression, while TNFSF14 showed higher expression in the low-risk subgroup.

The biological effects were confirmed through molecular biological experiments, as indicated by the aforementioned bioinformatic analysis. The gene expression of lncRNAs (NRAV, SNHG3, LINC00839 and AC004687.1) was investigated in both HCC cells and liver immortalized cells. The results revealed a significant upregulation of these lncRNAs in HCC cells compared to normal liver cells ($P < 0.05$), except for the downregulation in AC004687.1 (Fig. 9A). The Gefitinib treatment ($P < 0.05$) (Fig. 9B) was additionally confirmed by a biological functional assay to have inhibited the growth of HCC cells. In the meantime, the predictive lncRNAs was significantly depleted in comparison to the liver cells that were considered normal ($P < 0.05$), except for the upregulation in AC004687.1 (Fig. 9C). Thus, our data provided a promising reference for clinical therapy of HCC.

9. Discussion

In our study, we succeed to construct an ERS and cuproptosis-related lncRNA prognostic signature, including NRAV, SNHG3, LINC00839 and AC004687.1, which was used to divide into high- and low-risk groups in HCC patients. Survival and predictive performance, immunologic efficacy evaluations, drug sensitivity, and mutational status analysis were performed together for further exploration. Meanwhile, prognostic lncRNAs expression and proliferation in HCC cells were validated. There was a strong correlation between the signature and clinical characteristics, with an enrichment analysis showing that biological membrane pathways were enriched. HCC patients in low-risk exhibited lower TMB and higher immune status. A cluster analysis revealed that cluster 2 had the best clinical immunological efficacy and most active immune function.

In addition to protein-coding genes, the human genome also holds non-coding RNA, such as lncRNAs. According to prior research, it has been indicated that the modification of particular lncRNAs has expedited the advancement of tumors [43]. As part of our study, we incorporated four lncRNAs associated with ERS and cuproptosis into the prognostic signature, which were NRAV, SNHG3, LINC00839, and AC004687.1. Initially discovered as a traditional lncRNA, lncNRAV was observed to regulate antiviral reactions by inhibiting the transcription of interferon-stimulated genes [44]. Additionally, NRAV was proved to act as a vital regulator and biomarker in malignancy, especially HCC [45,46]. We noticed that NRAV could be the HCC prognostic biomarker of immune-related

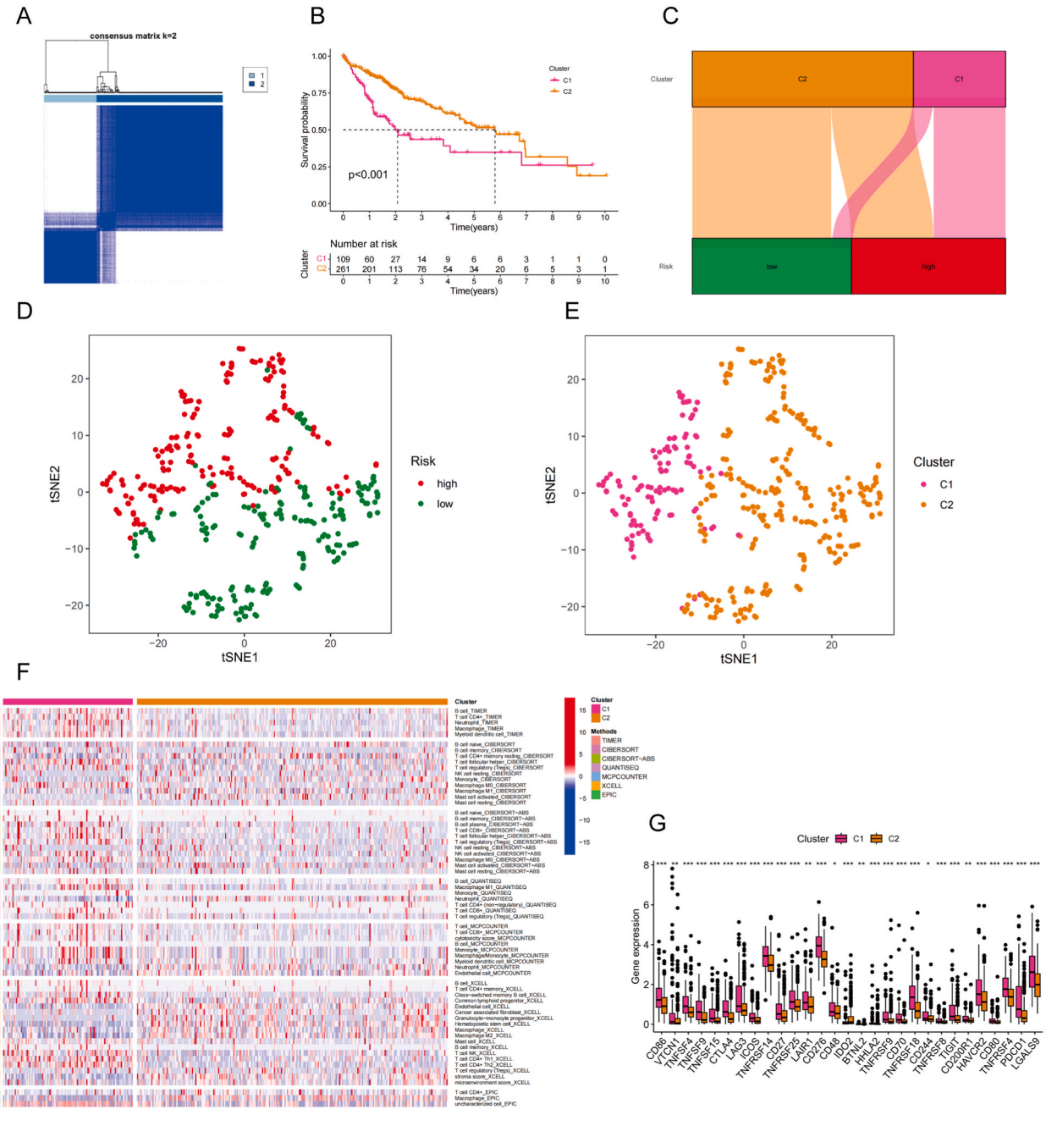

Fig. 7. Survival, tSNE, infiltrating immune cells and the expression of immune checkpoints in two distinct subgroups identified by consensus clustering.
(A) Optimized consensus matrix ($k = 2$). (B) Kaplan-Meier plot of two distinct subgroups identified by consensus clustering. (C) The relationship between two subgroups and risk score in Sankey diagram. tSNE analysis in two distinct subgroups (D) and different risk subgroups (E). (F) Correlation heatmap of infiltrating immune cells in two distinct subgroups. (G) Differential expression of 43 immune checkpoint genes in two distinct subgroups.

lncRNAs [47], ferroptosis-related lncRNAs [48], N7-Methylguanosine-related LncRNA [49] and etc. Furthermore, a recently analysis also highlighted the function of NRAV as a cuproptosis-related prognostic biomarker in HCC [50]. In this instance, our data demonstrated the involvement of ERS and cuproptosis in HCC, indicating that NRAV might have a significant impact on the regulation of HCC progression through these two mechanisms above. Together with the antiviral response of liver, we proposed that NRAV might be the extreme driver of HCC caused by viral hepatitis. SNHG3, originally considered as a competitive endogenous RNA (ceRNA), binds

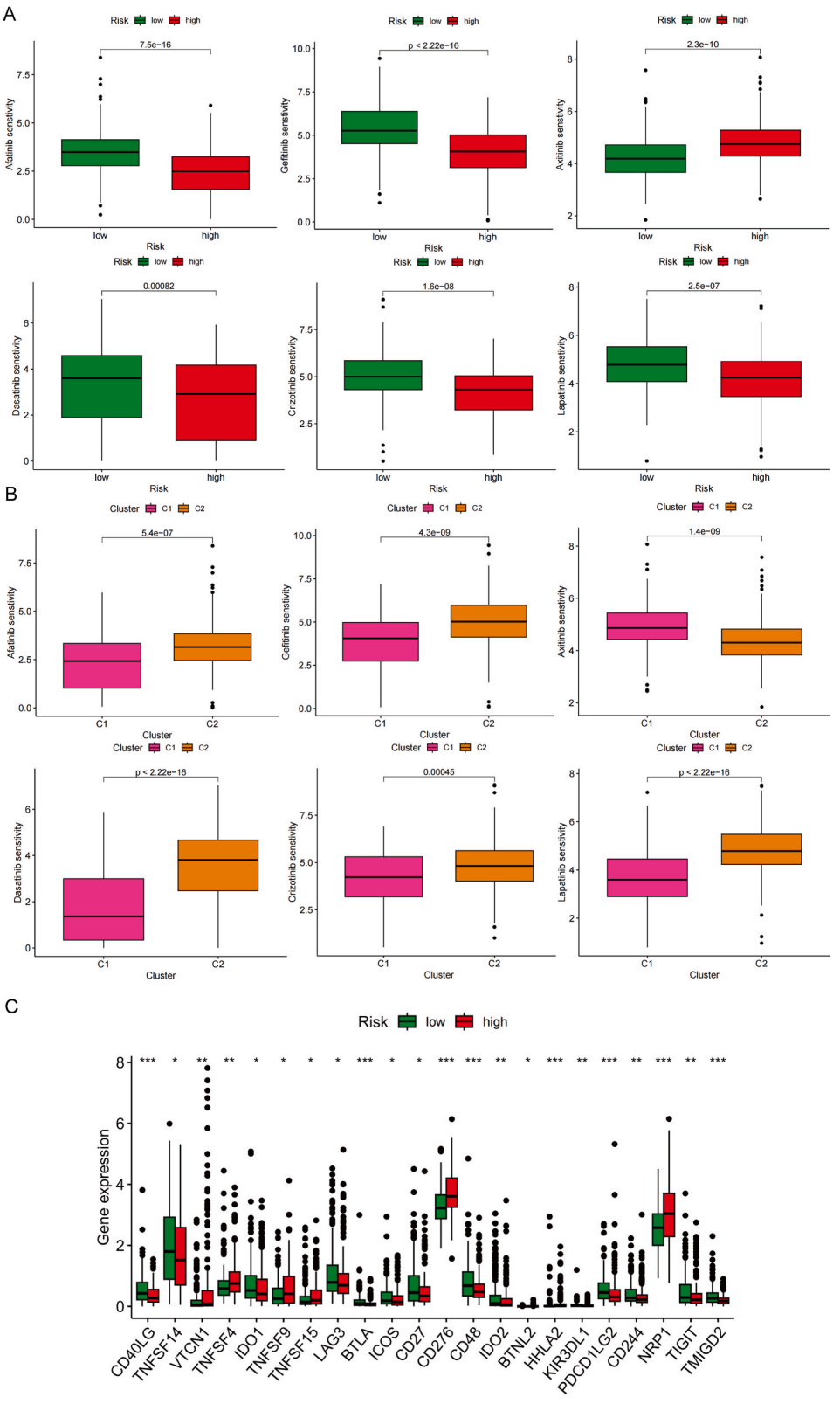

(caption on next page)

Fig. 8. Comparison of potential drugs sensitivity in different risk subgroups and clusters and the difference of immune checkpoint gene expression between two risk subgroups.
(A) The difference of potential drugs sensitivity between risk subgroups. (B) The difference of potential drugs sensitivity between distinct clusters. (C) The difference of immune checkpoint gene expression between two risk subgroups.

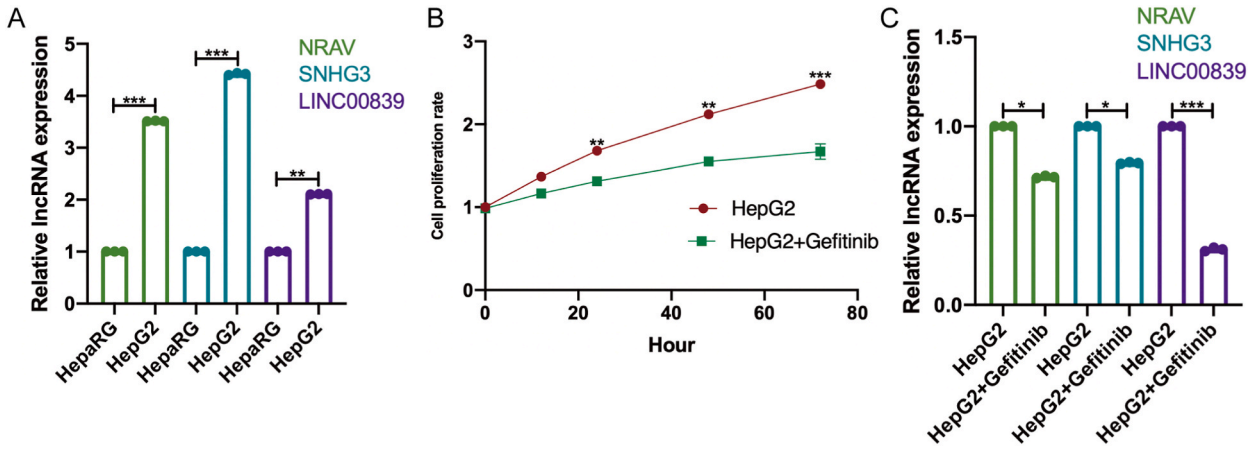

Fig. 9. The alteration of the prognostic lncRNAs expression and proliferation in HCC cells.
(A) The expression level of the prognostic lncRNAs. (B) The inhibition of Gefitinib on HepG2. (C) The expression level of the prognostic lncRNAs under the treatment of Gefitinib.

with tumor suppressor microRNAs [51]. The oncogenic role of SNHG3 in various malignancies has been further supported by emerging evidence [52], and SNHG3 has been found to contribute to drug resistance, proliferation, and invasion in tumors [53–55]. In the study by Hao et al. they developed a prognostic model for m6A methylation [56], in which SNHG3 was identified as one of the risk factors. Our data confirmed the feasibility of SNHG3 as a biomarker as well. In this context, we took into account that SNHG3 continued to focus on the miRNAs downstream to disrupt the regular signaling pathway in HCC. LINC00839, as a novel lncRNA, was discovered and named recently [57]. The newly research indicated that LINC00839 can influence the survival, spread, programmed cell death, movement, and infiltration in cancers [58,59], indicating its role in promoting carcinogenesis. It is also worth noting that a recent study reported LINC00839 as an m6A-enriched lncRNA that would promote the progression of nasopharyngeal carcinoma via transcriptional regulation of amine oxidase copper-containing 1 (AOC1) [60]. The recruitment of TATA-box binding protein associated factor (TAF15) to the promoter region of AOC1 was coordinated by the interaction between LINC00839 and TAF15, which enhanced the transcription of AOC1 and tumor progression. Though the direct relationship among LINC00839, AOC1, and HCC remains unclear, the AOC1 is already identified as a cuproptosis-related gene in HCC [61]. The AOC1 levels in HCC tumor tissues were up-regulated and related to poor prognosis. Furthermore, NRAV, SNHG3, and LINC00839 exhibited elevated mRNA expression in HCC cells and AC004687.1 had a downregulated expression, indicating their diagnostic significance in HCC. Notably, although AC004687.1 has not yet been officially named, our data suggested that AC004687.1 might act as an anti-oncogene and this was the first time that the expression of AC004687.1 and its relationship with HCC have been verified. Nevertheless, the specific mechanisms in malignancies, especially HCC, remain unclear. To sum up, our data elucidated the possibility of those prognostic lncRNAs to apply to be biomarkers.

During the analysis of downstream mechanism enrichment, genes related to ERS and cuproptosis showed significant enrichment in the biological processes of cell recognition, phagocytosis, and completement activation. They were also enriched in cellular components such as the external side of the plasma membrane, immunoglobulin complex, and condensed chromosome. Additionally, these genes exhibited molecular functions like antigen binding and immunoglobulin receptor binding. It's common knowledge that cell identification and engulfment played a role in the transfer of cytomembrane constituents, encompassing cytomembrane and endoplasmic reticulum. Furthermore, the molecular function of antigen binding or immunoglobulin receptor binding requires the involvement of the endoplasmic reticulum for proper protein folding. The findings of cellular structure indicated that the transfer of organic membrane could potentially occur in ERS. Therefore, lncRNAs associated with ERS and cuproptosis, which include the lncRNAs that predict risk prognosis, could potentially be involved in the regulation of protein processing by influencing the exchange of biological membrane. Next, we analyzed that the downstream signaling pathways in GSEA were involved in ECM-related signaling pathways, Notch signaling pathway, ligand and receptor interaction pathway and etc. In their study, Zhang and colleagues discovered that orientin reduced oxidative stress-induced ERS and mitochondrial dysfunction in rat nucleus pulposus cells through the AMPK/SIRT1 pathway. They also observed a decrease in intervertebral disc degeneration in vivo [62]. Furthermore, Suo and colleagues demonstrated that Hsa_circ_0056686, originating from cancer-related fibroblasts within the extracellular matrix, enhances cellular growth and inhibits programmed cell death in uterine leiomyoma by blocking ERS [63]. The connection between ECM and ERS was examined in both cancerous and noncancerous conditions. The disrupted balance of ECM frequently initiates a series of pathological processes that promote the development of tumors, and the formation of tumors also contributes to additional ECM imbalances [64].

Meanwhile, the Notch signaling pathway was considered as the key pathway to regulate the biological function of macrophages [65]. In their study, Koike and colleagues discovered that the expansion of cumulus-oocyte complex in polycystic ovary syndrome was regulated by the Notch signaling pathway activated by ERS [65]. In cultured GLCs, the expression of Notch2 and Notch-target transcription factors could be increased by ERS. In their study, Dai and colleagues discovered that suppressing Angiopoietin-2 relieved inflammation, barrier dysfunction, and ERS in intestinal epithelial cells caused by lipopolysaccharide. This was achieved by inhibiting the Notch signaling pathway [65]. Recent studies have demonstrated the connection between the Notch signaling pathway and ERS. Based on the latest findings and previous studies, the prognostic risk signature has the potential to trigger changes in the ECM or modify the ECM, while also interacting with the Notch signaling pathway in HCC, either directly or indirectly. Based on those discoveries, we anticipate that future research will provide a more detailed understanding of the ERS mechanism.

Additionally, the genetic characteristics and tumor microenvironment of the prognostic model were also investigated. We found that most mutations occurred in high-risk groups, while CSMD3 (9 %) showed a remarkably higher prevalence in low-risk groups. There was few evidence to prove the regulatory mechanism between CSMD3 mutation and ERS. Therefore, ERS has the potential to greatly enhance the occurrence rate of HCC mutations, although it does not have a substantial impact on the specific mutation types. The presence of gene mutation was frequently linked to higher TMB and enhances the body's ability to fight against tumors. These observed variations in mutations could potentially act as a biomarker for predicting immune response. Additionally, we observed that patients in the high-TBM group had the lowest likelihood of survival, suggesting that TBM may serve as a distinct factor in analyzing survival due to its potential influence on immune status. To verify the potential of the risk prognostic signature in clinical therapy, an analysis was conducted to assess the sensitivity of traditional target medications. The low-risk subgroup achieved a higher level of susceptibility. Additionally, the robust predictive significance was confirmed by various risk subcategories and unique groupings. Although there was difference in methods, the sensitivity of drugs remained uniform on the basis of above results. Choosing appropriate medications through the creation of enhanced screening methods remains a challenge due to the limited availability and specific requirements of targeted therapeutic drugs for HCC. Afatinib, Gefitinib, Axitinib, Dasatinib, Crizotinib and Lapatinib were primary antitumor target drugs and represented distinct pharmacologic action. Dasatinib, Crizotinib and Lapatinib were inhibitor of multiple tyrosine kinases, ATP-competitive small-molecule inhibitor of the receptor tyrosine kinases (RTK) C-Met, ALK and ROS1 and tyrosine kinase inhibitor targeting epidermal growth factor receptor (EGFR) and HER2, respectively [66,67], which were applied to the development of treatment in HCC cells and resulted in effective treatment responsiveness [68,69]. Afatinib, Axitinib, and Gefitinib are classified as inhibitors of EGFR or VEGR, and there were still numerous shortcomings in the research regarding the impact of Gefitinib on HCC [70–72]. Although Gefitinib has not yet been formally used in HCC patients, relevant studies in vivo are ongoing [73]. At present, we have verified the efficacy of Gefitinib in vivo. The application of Gefitinib led to a notable reduction in the cellular vitality of HCC cells, while also inhibiting the expression of high-risk prognostic lncRNAs. This finding serves as additional evidence supporting the potential use of Gefitinib in treating HCC. While the precise mechanisms underlying each component of the model linked to HCC remain unidentified, our study offers insights to clinicians for additional research on mechanisms and the development of clinical drugs. There are also some shortcomings in our study. Firstly, our results were performed based on public database and lack the validation from our independent cohort. Secondly, the potential mechanisms and immune status in high- and low-risk subgroups were explored and further need to be supported via the results of molecular biology. More investigations will be initiated based on the present conclusions in this study.

10. Conclusion

To summarize, based on the 4 screened lncRNAs related to ERS and cuproptosis, we developed a prognostic signature for ERS and cuproptosis-related lncRNA risk. This signature identified 2 subgroups with distinct prognostic features and revealed the correlation with immune response, tumor mutational burden (TMB), and various clinical therapies including targeted therapy, immunotherapy and chemotherapy. The present finding offers a valuable guide for potential medical practice and eventually benefits the prognosis of HCC patients.

Consent for publication

It is not applicable.

Availability of data and materials

The data sets supporting the results of this article are included within the article.

Ethics approval and consent to participate

Not applicable.

Funding

This work was supported by The National Natural Science Foundation of China (No. 82100639, 81970526). Shanghai Science and Technology Program (22015830900) and Natural Science Foundation of Xinjiang Uygur Autonomous Region (2022D01F17).

CRediT authorship contribution statement

Xiao-Liang Qi: Writing – original draft. **Gu-Qing Luo:** Investigation. **Abudukadier Tuersun:** Software. **Min Chen:** Methodology. **Guang-Bo Wu:** Supervision. **Lei Zheng:** Visualization. **Hong-Jie Li:** Formal analysis. **Xiao-Lou Lou:** Conceptualization. **Meng Luo:** Funding acquisition.

Declaration of competing interest

The authors declare that they have no known competing financial interests or personal relationships that could have appeared to influence the work reported in this paper.

Acknowledgements

Not applicable.

Abbreviation list

TMB Tumor mutational burden
LASSO Least absolute shrinkage, and selection operator
ESTIMATE Estimation of STromal and Immune cells in MAlignant Tumor tissues using Expression
TIDE Tumor immune dysfunction and exclusion
ERS Endoplasmic reticulum stress
TCGA the Cancer Genome Atlas
GSEA Gene Set Enrichment Analysis
KEGG Kyoto Encyclopedia of Genes and Genomes
GO Gene ontology
HR Hazard Rates
PCGProtein-coding Genes.

Appendix A. Supplementary data

Supplementary data to this article can be found online at https://doi.org/10.1016/j.heliyon.2024.e38342.

References

[1] Hepatocellular carcinoma, Nat. Rev. Dis. Prim. 7 (1) (2021) 7.
[2] A. Forner, M. Reig, J. Bruix, Hepatocellular carcinoma, Lancet 391 (10127) (2018) 1301–1314.
[3] P. Fagone, S. Jackowski, Membrane phospholipid synthesis and endoplasmic reticulum function, JLR (J. Lipid Res.) 50 (2009) S311–S316. Suppl(Suppl).
[4] Y. Ma, L.M. Hendershot, ER chaperone functions during normal and stress conditions, J. Chem. Neuroanat. 28 (1–2) (2004) 51–65.
[5] J. He, G. Li, X. Liu, L. Ma, P. Zhang, J. Zhang, et al., Diagnostic and prognostic values of MANF expression in hepatocellular carcinoma, BioMed Res. Int. 2020 (2020) 1936385.
[6] H. Xu, Y. Tian, D. Tang, S. Zou, G. Liu, J. Song, et al., An endoplasmic reticulum stress-MicroRNA-26a feedback circuit in NAFLD, Hepatology 73 (4) (2021) 1327–1345.
[7] P. Wadgaonkar, F. Chen, Connections between endoplasmic reticulum stress-associated unfolded protein response, mitochondria, and autophagy in arsenic-induced carcinogenesis, Semin. Cancer Biol. 76 (2021) 258–266.
[8] S.J. Marciniak, J.E. Chambers, D. Ron, Pharmacological targeting of endoplasmic reticulum stress in disease, Nat. Rev. Drug Discov. 21 (2) (2022) 115–140.
[9] C. Atkins, Q. Liu, E. Minthorn, S.-Y. Zhang, D.J. Figueroa, K. Moss, et al., Characterization of a novel PERK kinase inhibitor with antitumor and antiangiogenic activity, Cancer Res. 73 (6) (2013) 1993–2002.
[10] J. Wu, S. Qiao, Y. Xiang, M. Cui, X. Yao, R. Lin, et al., Endoplasmic reticulum stress: multiple regulatory roles in hepatocellular carcinoma, Biomed. Pharmacother. 142 (2021) 112005.
[11] P. Tsvetkov, S. Coy, B. Petrova, M. Dreishpoon, A. Verma, M. Abdusamad, et al., Copper induces cell death by targeting lipoylated TCA cycle proteins, Science (New York, NY) 375 (6586) (2022) 1254–1261.
[12] Y. Wang, L. Zhang, F. Zhou, Cuproptosis: a new form of programmed cell death, Cell. Mol. Immunol. 19 (8) (2022) 867–868.
[13] Y. Liao, J. Zhao, K. Bulek, F. Tang, X. Chen, G. Cai, et al., Inflammation mobilizes copper metabolism to promote colon tumorigenesis via an IL-17-STEAP4-XIAP axis, Nat. Commun. 11 (1) (2020) 900.
[14] J. Guo, J. Cheng, N. Zheng, X. Zhang, X. Dai, L. Zhang, et al., Copper promotes tumorigenesis by activating the PDK1-AKT oncogenic pathway in a copper transporter 1 dependent manner, Adv. Sci. 8 (18) (2021) e2004303.
[15] P. Zheng, C. Zhou, L. Lu, B. Liu, Y. Ding, Elesclomol: a copper ionophore targeting mitochondrial metabolism for cancer therapy, J. Exp. Clin. Cancer Res. : CR 41 (1) (2022) 271.
[16] Z. Zhang, X. Zeng, Y. Wu, Y. Liu, X. Zhang, Z. Song, Cuproptosis-related risk score predicts prognosis and characterizes the tumor microenvironment in hepatocellular carcinoma, Front. Immunol. 13 (2022) 925618.
[17] G. Zhang, J. Sun, X. Zhang, A novel Cuproptosis-related LncRNA signature to predict prognosis in hepatocellular carcinoma, Sci. Rep. 12 (1) (2022) 11325.
[18] L. Kong, H. Huang, S. Luan, H. Liu, M. Ye, F. Wu, Inhibition of ASIC1a-mediated ERS improves the activation of HSCs and copper transport under copper load, Front. Pharmacol. 12 (2021) 653272.
[19] S. Ma, Y. Liu, C. Zhao, P. Chu, S. Yin, T. Wang, Copper induced intestinal inflammation response through oxidative stress induced endoplasmic reticulum stress in Takifugu fasciatus, Aquatic toxicology (Amsterdam, Netherlands) 261 (2023) 106634.

[20] J. Guo, Y. Bai, J. Liao, S. Wang, Q. Han, Z. Tang, Copper induces apoptosis through endoplasmic reticulum stress in skeletal muscle of broilers, Biol. Trace Elem. Res. 198 (2) (2020) 636–643.
[21] D. Li, C. Yang, C. Yin, F. Zhao, Z. Chen, Y. Tian, et al., LncRNA, important player in bone development and disease, Endocr., Metab. Immune Disord.: Drug Targets 20 (1) (2020) 50–66.
[22] X. Qian, J. Zhao, P.Y. Yeung, Q.C. Zhang, C.K. Kwok, Revealing lncRNA structures and interactions by sequencing-based approaches, Trends Biochem. Sci. 44 (1) (2019) 33–52.
[23] Z. Ma, J. Zhang, X. Xu, Y. Qu, H. Dong, J. Dang, et al., LncRNA expression profile during autophagy and Malat1 function in macrophages, PLoS One 14 (8) (2019) e0221104.
[24] Y. Lin, Y. Shen, J. Chen, C. Hu, Z. Zhou, C. Yuan, The function of LncRNA FTX in several common cancers, Curr. Pharmaceut. Des. 27 (20) (2021) 2381–2386.
[25] J. Li, J. Xie, Y.-Z. Wang, Y.-R. Gan, L. Wei, G.-W. Ding, et al., Overexpression of lncRNA Dancr inhibits apoptosis and enhances autophagy to protect cardiomyocytes from endoplasmic reticulum stress injury via sponging microRNA-6324, Mol. Med. Rep. 23 (2) (2021).
[26] G. Wang, Q. Ye, S. Ning, Z. Yang, Y. Chen, L. Zhang, et al., LncRNA MEG3 promotes endoplasmic reticulum stress and suppresses proliferation and invasion of colorectal carcinoma cells through the MEG3/miR-103a-3p/PDHB ceRNA pathway, Neoplasma 68 (2) (2021) 362–374.
[27] K.L. Howe, P. Achuthan, J. Allen, J. Allen, J. Alvarez-Jarreta, M.R. Amode, et al., Ensembl 2021, Nucleic Acids Res. 49 (D1) (2021) D884–D891.
[28] G. Stelzer, N. Rosen, I. Plaschkes, S. Zimmerman, M. Twik, S. Fishilevich, et al., The GeneCards suite: from gene data mining to disease genome sequence analyses, Curr Protoc Bioinformatics 54 (2016).
[29] B. Deng, F. Liao, Y. Liu, P. He, S. Wei, C. Liu, et al., Comprehensive analysis of endoplasmic reticulum stress-associated genes signature of ulcerative colitis, Front. Immunol. 14 (2023) 1158648.
[30] P. Chen, J. Yu, Q. Luo, J. Li, W. Wang, Construction of disulfidptosis-related lncRNA signature for predicting the prognosis and immune escape in colon adenocarcinoma, BMC Gastroenterol. 23 (1) (2023) 382.
[31] Y. Gao, Z. Jia, Prognosis signature of cuprotosis-related lncRNAs associated with kidney renal clear cell carcinoma, Genet. Res. 2022 (2022) 6004852.
[32] W. Li, G. Yang, H. Dong, J. Zhu, T. Liu, A prognostic signature based on cuprotosis-related long non-coding RNAs predicts the prognosis and sensitivity to chemotherapy in patients with colorectal cancer, Front. Med. 9 (2022) 1055785.
[33] A.-A. Li, F. Li, M. Lan, Y. Zhang, D. Xie, M.-Y. Yan, A novel endoplasmic reticulum stress-related lncRNA prognostic risk model for cutaneous melanoma, J. Cancer Res. Clin. Oncol. 148 (12) (2022) 3227–3241.
[34] Y. Zheng, X. Yue, C. Fang, Z. Jia, Y. Chen, H. Xie, et al., A novel defined endoplasmic reticulum stress-related lncRNA signature for prognosis prediction and immune therapy in glioma, Front. Oncol. 12 (2022) 930923.
[35] S.I. Vrieze, Model selection and psychological theory: a discussion of the differences between the Akaike information criterion (AIC) and the Bayesian information criterion (BIC), Psychol. Methods 17 (2) (2012) 228–243.
[36] C. Yang, X. Huang, Z. Liu, W. Qin, C. Wang, Metabolism-associated molecular classification of hepatocellular carcinoma, Mol. Oncol. 14 (4) (2020) 896–913.
[37] A.J. Gentles, A.M. Newman, C.L. Liu, S.V. Bratman, W. Feng, D. Kim, et al., The prognostic landscape of genes and infiltrating immune cells across human cancers, Nat. Med. 21 (8) (2015) 938–945.
[38] P. Jiang, S. Gu, D. Pan, J. Fu, A. Sahu, X. Hu, et al., Signatures of T cell dysfunction and exclusion predict cancer immunotherapy response, Nat. Med. 24 (10) (2018) 1550–1558.
[39] Y. Hoshida, J.-P. Brunet, P. Tamayo, T.R. Golub, J.P. Mesirov, Subclass mapping: identifying common subtypes in independent disease data sets, PLoS One 2 (11) (2007) e1195.
[40] M.-J. Marion, O. Hantz, D. Durantel, The HepaRG cell line: biological properties and relevance as a tool for cell biology, drug metabolism, and virology studies, Methods Mol. Biol. 640 (2010) 261–272.
[41] M.T. Donato, L. Tolosa, M.J. Gómez-Lechón, Culture and functional characterization of human hepatoma HepG2 cells, Methods Mol. Biol. 1250 (2015) 77–93.
[42] T.G. Gabig, W.C. Waltzer, T. Whyard, V. Romanov, Clostridium perfringens enterotoxin as a potential drug for intravesical treatment of bladder cancer, Biochem. Biophys. Res. Commun. 478 (2) (2016) 887–892.
[43] E.S. Martens-Uzunova, R. Böttcher, C.M. Croce, G. Jenster, T. Visakorpi, G.A. Calin, Long noncoding RNA in prostate, bladder, and kidney cancer, Eur. Urol. 65 (6) (2014) 1140–1151.
[44] J. Ouyang, X. Zhu, Y. Chen, H. Wei, Q. Chen, X. Chi, et al., NRAV, a long noncoding RNA, modulates antiviral responses through suppression of interferon-stimulated gene transcription, Cell Host Microbe 16 (5) (2014) 616–626.
[45] A. Nicknam, S. Khojasteh Pour, M.A. Hashemnejad, B.M. Hussen, A. Safarzadeh, S. Eslami, et al., Expression analysis of Rho GTPase-related lncRNAs in breast cancer, Pathol. Res. Pract. 244 (2023) 154429.
[46] Q. Wang, Y. Tang, Y. Ge, S. Zhang, M. Zheng, Long non-coding RNA NRAV enhances proliferation and invasion of hepatocellular carcinoma cells by modulating the Wnt/β-catenin signaling pathway, Bioengineered 13 (4) (2022) 10026–10037.
[47] Q. Xu, Y. Wang, W. Huang, Identification of immune-related lncRNA signature for predicting immune checkpoint blockade and prognosis in hepatocellular carcinoma, Int. Immunopharm. 92 (2021) 107333.
[48] Z.-A. Chen, H. Tian, D.-M. Yao, Y. Zhang, Z.-J. Feng, C.-J. Yang, Identification of a ferroptosis-related signature model including mRNAs and lncRNAs for predicting prognosis and immune activity in hepatocellular carcinoma, Front. Oncol. 11 (2021) 738477.
[49] C. Yang, L. Zhang, X. Hao, M. Tang, B. Zhou, J. Hou, Identification of a novel N7-methylguanosine-related LncRNA signature predicts the prognosis of hepatocellular carcinoma and experiment verification, Curr. Oncol. 30 (1) (2022) 430–448.
[50] H. Peng, Z. Zou, Z. Xiang, X. Lu, Y. Zhang, X. Peng, Cuproptosis-related prognostic signatures predict the prognosis and immunotherapy in HCC patients, Medicine 102 (34) (2023) e34741.
[51] B. Xu, J. Mei, W. Ji, Z. Bian, J. Jiao, J. Sun, et al., LncRNA SNHG3, a potential oncogene in human cancers, Cancer Cell Int. 20 (1) (2020) 536.
[52] T. Li, Y. Xing, F. Yang, Y. Sun, S. Zhang, Q. Wang, et al., LncRNA SNHG3 sponges miR-577 to up-regulate SMURF1 expression in prostate cancer, Cancer Med. 9 (11) (2020) 3852–3862.
[53] P.-F. Zhang, F. Wang, J. Wu, Y. Wu, W. Huang, D. Liu, et al., LncRNA SNHG3 induces EMT and sorafenib resistance by modulating the miR-128/CD151 pathway in hepatocellular carcinoma, J. Cell. Physiol. 234 (3) (2019) 2788–2794.
[54] F. Zhang, J. Lu, J. Yang, Q. Dai, X. Du, Y. Xu, et al., SNHG3 regulates NEIL3 via transcription factor E2F1 to mediate malignant proliferation of hepatocellular carcinoma, Immunogenetics 75 (1) (2023) 39–51.
[55] J. Wu, L. Liu, H. Jin, Q. Li, S. Wang, B. Peng, LncSNHG3/miR-139-5p/BMI1 axis regulates proliferation, migration, and invasion in hepatocellular carcinoma, OncoTargets Ther. 12 (2019) 6623–6638.
[56] H. Yang, H. Yang, W. Zhang, J. Wang, L. Sun, J. Gao, et al., Identification of m6A-related lncRNA to predict the prognosis of patients with hepatocellular carcinoma, BioMed Res. Int. 2022 (2022) 4169150.
[57] Q. Zhang, J. Wei, N. Li, B. Liu, LINC00839 promotes neuroblastoma progression by sponging miR-454-3p to up-regulate NEUROD1, Neurochem. Res. 47 (8) (2022) 2278–2293.
[58] X. Yu, Y. Jiang, X. Hu, X. Ge, LINC00839/miR-519d-3p/JMJD6 axis modulated cell viability, apoptosis, migration and invasiveness of lung cancer cells, Folia Histochem. Cytobiol. 59 (4) (2021) 271–281.
[59] X. Zhou, Y. Chang, L. Zhu, C. Shen, J. Qian, R. Chang, LINC00839/miR-144-3p/WTAP (WT1 Associated protein) axis is involved in regulating hepatocellular carcinoma progression, Bioengineered 12 (2) (2021) 10849–10861.
[60] W.H. Zheng, Z.Q. Long, Z.Q. Zheng, L.L. Zhang, Y.L. Liang, Z.X. Li, et al., m6A-enriched lncRNA LINC00839 promotes tumor progression by enhancing TAF15-mediated transcription of amine oxidase AOC1 in nasopharyngeal carcinoma, J. Biol. Chem. 299 (7) (2023) 104873.
[61] X. Zhao, J. Chen, S. Yin, J. Shi, M. Zheng, C. He, et al., The expression of cuproptosis-related genes in hepatocellular carcinoma and their relationships with prognosis, Front. Oncol. 12 (2022) 992468.

[62] Z. Zhang, J. Wu, C. Teng, J. Wang, J. Yu, C. Jin, et al., Orientin downregulating oxidative stress-mediated endoplasmic reticulum stress and mitochondrial dysfunction through AMPK/SIRT1 pathway in rat nucleus pulposus cells in vitro and attenuated intervertebral disc degeneration in vivo, Apoptosis 27 (11–12) (2022) 1031–1048.
[63] M. Suo, Z. Lin, D. Guo, A. Zhang, Hsa_circ_0056686, derived from cancer-associated fibroblasts, promotes cell proliferation and suppresses apoptosis in uterine leiomyoma through inhibiting endoplasmic reticulum stress, PLoS One 17 (4) (2022) e0266374.
[64] M. Najafi, B. Farhood, K. Mortezaee, Extracellular matrix (ECM) stiffness and degradation as cancer drivers, J. Cell. Biochem. 120 (3) (2019) 2782–2790.
[65] W. Chen, Y. Liu, J. Chen, Y. Ma, Y. Song, Y. Cen, et al., The Notch signaling pathway regulates macrophage polarization in liver diseases, Int. Immunopharm. 99 (2021) 107938.
[66] M. Voigtlaender, T. Schneider-Merck, M. Trepel, Lapatinib. Recent results, Cancer Res. 211 (2018) 19–44.
[67] M. Shao, R. Shi, Z.-X. Gao, S.-S. Gao, J.-F. Li, H. Li, et al., Crizotinib and doxorubicin cooperatively reduces drug resistance by mitigating MDR1 to increase hepatocellular carcinoma cells death, Front. Oncol. 11 (2021) 650052.
[68] Z. Cheng, H. Huang, M. Li, X. Liang, Y. Tan, Y. Chen, Lactylation-related gene signature effectively predicts prognosis and treatment responsiveness in hepatocellular carcinoma, Pharmaceuticals 16 (5) (2023).
[69] I. El Sayed, M.W. Helmy, H.S. El-Abhar, Inhibition of SRC/FAK cue: a novel pathway for the synergistic effect of rosuvastatin on the anti-cancer effect of dasatinib in hepatocellular carcinoma, Life Sci. 213 (2018) 248–257.
[70] A.S. Bodzin, Z. Wei, R. Hurtt, T. Gu, C. Doria, Gefitinib resistance in HCC mahlavu cells: upregulation of CD133 expression, activation of IGF-1R signaling pathway, and enhancement of IGF-1R nuclear translocation, J. Cell. Physiol. 227 (7) (2012) 2947–2952.
[71] C. Yu, X. Zhang, M. Wang, G. Xu, S. Zhao, Y. Feng, et al., Afatinib combined with anti-PD1 enhances immunotherapy of hepatocellular carcinoma via ERBB2/STAT3/PD-L1 signaling, Front. Oncol. 13 (2023) 1198118.
[72] H. Jiang, J. Liao, L. Wang, C. Jin, J. Mo, S. Xiang, The multikinase inhibitor axitinib in the treatment of advanced hepatocellular carcinoma: the current clinical applications and the molecular mechanisms, Front. Immunol. 14 (2023) 1163967.
[73] H. Jin, Y. Shi, Y. Lv, S. Yuan, C.F.A. Ramirez, C. Lieftink, et al., EGFR activation limits the response of liver cancer to lenvatinib, Nature 595 (7869) (2021) 730–734.